Assessment of the structural brain network reveals altered connectivity in children with unilateral cerebral palsy due to periventricular white matter lesions

Kerstin Pannek [a,b,c], Roslyn N. Boyd [a], Simona Fiori [d], Andrea Guzzetta [d,e], Stephen E. Rose [c,*]

[a] The University of Queensland, Queensland Cerebral Palsy and Rehabilitation Research Centre, Brisbane, Australia
[b] The University of Queensland, School of Medicine, Brisbane, Australia
[c] The Australian e-Health Research Centre, CSIRO, Brisbane, Australia
[d] Stella Maris Scientific Institute, Pisa, Italy
[e] Department of Clinical and Experimental Medicine, University of Pisa, Italy

ARTICLE INFO

ABSTRACT

Background: Cerebral palsy (CP) is a term to describe the spectrum of disorders of impaired motor and sensory function caused by a brain lesion occurring early during development. Diffusion MRI and tractography have been shown to be useful in the study of white matter (WM) microstructure in tracts likely to be impacted by the static brain lesion.
Aim: The purpose of this study was to identify WM pathways with altered connectivity in children with unilateral CP caused by periventricular white matter lesions using a whole-brain connectivity approach.
Methods: Data of 50 children with unilateral CP caused by periventricular white matter lesions (5–17 years; manual ability classification system [MACS] I = 25/II = 25) and 17 children with typical development (CTD; 7–16 years) were analysed. Structural and High Angular Resolution Diffusion weighted Images (HARDI; 64 directions, b = 3000 s/mm^2) were acquired at 3 T. Connectomes were calculated using whole-brain probabilistic tractography in combination with structural parcellation of the cortex and subcortical structures. Connections with altered fractional anisotropy (FA) in children with unilateral CP compared to CTD were identified using network-based statistics (NBS). The relationship between FA and performance of the impaired hand in bimanual tasks (Assisting Hand Assessment—AHA) was assessed in connections that showed significant differences in FA compared to CTD.
Results: FA was reduced in children with unilateral CP compared to CTD. Seven pathways, including the corticospinal, thalamocortical, and fronto-parietal association pathways were identified simultaneously in children with left and right unilateral CP. There was a positive relationship between performance of the impaired hand in bimanual tasks and FA within the cortico-spinal and thalamo-cortical pathways ($r^2 = 0.16$–0.44; $p < 0.05$).
Conclusion: This study shows that network-based analysis of structural connectivity can identify alterations in FA in unilateral CP, and that these alterations in FA are related to clinical function. Application of this connectome-based analysis to investigate alterations in connectivity following treatment may elucidate the neurological correlates of improved functioning due to intervention.

1. Introduction

Cerebral palsy (CP) has been defined as "a group of permanent disorders of the development of movement and posture, causing activity limitation, that are attributed to non-progressive disturbances that occurred in the developing foetal or infant brain" (Rosenbaum et al., 2007). It is a condition with myriad clinical manifestations and functional limitations. Structural magnetic resonance imaging (MRI), such as T1- or T2-weighted imaging, can be used to assess the location and size of brain lesions in children with cerebral palsy, and can be used to

elucidate the aetiology or pathogenesis of CP (Krägeloh-Mann and Horber, 2007). It is, however, difficult to establish a relationship between structural MRI and clinical function (Arnfield et al., 2013). While larger brain lesions typically indicate higher severity of impairments, similarly severe impairments can be seen in children with small lesions in functionally relevant areas or even in those with apparently normal structural MRI (Krägeloh-Mann and Horber, 2007; Miller, 2005). An assessment of the microstructural properties of the white matter is therefore required for an improved understanding of the relationship between brain microstructure and clinical function.

Diffusion MRI provides a non-invasive tool to probe white matter microstructure. The diffusion of water molecules in the brain is hindered and restricted by the presence of axons in the brain. Changes in water diffusion are associated with changes in myelination, axon density and diameter, and coherence (Scholz et al., 2009). Tissue microstructural properties are frequently characterised using the quantitative diffusion metrics fractional anisotropy (FA) and mean diffusivity (MD); see Basser and Ozarslan (2010) for a review. In addition, diffusion MRI allows the delineation of white matter pathways by tractography, and subsequent assessment of microstructure within three-dimensional tracts rather than two-dimensional regions of interest. Both diffusion MRI and tractography have previously been used to investigate CP in paediatric populations (see Scheck et al., 2012 for a systematic review).

Perhaps not surprisingly, the corticospinal tract – the major descending motor pathway in the brain – has been the most frequent target of tractography investigations in CP (Chang et al., 2012; Chaturvedi et al., 2012; Glenn et al., 2007; Holmström et al., 2011; Hoon et al., 2002; Koerte et al., 2011; Rha et al., 2012; Rose et al., 2011; Son et al., 2007, 2009; Thomas et al., 2005; Trivedi et al., 2010; Yoshida et al., 2010), with a recently increased interest in ascending sensory pathways (Chaturvedi et al., 2012; Hoon et al., 2002; Rha et al., 2012; Rose et al., 2011; Thomas et al., 2005; Trivedi et al., 2010; Yoshida et al., 2010). Other projection, association and commissural pathways have been investigated less frequently (Koerte et al., 2011; Thomas et al., 2005). In the majority of these studies, the identification of pathways associated with CP was limited by the use of the diffusion tensor model to drive tractography, as well as the necessity of a priori hypotheses concerning the pathways to be investigated.

The aim of this study was to identify pathways associated with unilateral cerebral palsy from the structural network of connections in an automated fashion. This approach requires no a priori hypotheses regarding the tracts of interest, and has the potential of identifying pathways of altered microstructure that were not previously investigated in unilateral CP. To achieve this, we calculated the structural connectomes of children with unilateral left and right CP caused by periventricular white matter (PWM) lesions, as well as children with typical development (CTD) using High Angular Resolution Diffusion Imaging (HARDI) tractography, and investigated differences in FA between participant groups using a network-based statistics approach. We further hypothesised that a relationship would exist between FA of the identified pathways and performance of the impaired hand in bimanual tasks.

2. Methods

2.1. Participants

Study participants included children who were recruited and assessed at baseline as part of ongoing cohort studies of children with unilateral CP at our centre, investigating executive function (Bodimeade et al., 2013), the effect of web-based multimodal training (Mitii) (Boyd et al., 2013a), and the effect of constraint induced movement and bimanual therapy (CoMBiT) (Boyd et al., 2013b) on brain structure and function in children and adolescents with unilateral CP. Children with mild to moderate unilateral CP (congenital spastic hemiplegia; Gross Motor Function Classification System I–II, Manual Ability Classification System I–II), aged between 5 and 18 years, with sufficient cooperation and cognitive understanding to participate in therapy activities (Boyd et al., 2013a,b), and no contraindication for MRI and no epilepsy were eligible for recruitment.

A total of 80 children with unilateral CP (age 5–17 years), of whom 38 presented with left unilateral CP and 42 presented with right unilateral CP, as well as 21 children with typical development (CTD, age 7–16 years) recruited from the community with no indication for brain MRI participated in one or more of the abovementioned studies and had MRI performed at baseline (see Table 1 for participant demographics).

The University of Queensland and Children's Health Queensland ethics committees granted ethical approval. Informed parental consent was obtained from all participants.

2.2. Clinical testing

Performance of the impaired hand in bimanual tasks was assessed using the Assisting Hand Assessment (AHA; (Krumlinde-Sundholm and Eliasson, 2003)). The AHA assesses the effectiveness with which a child uses their impaired hand in bimanual activities. The school kids version of the AHA has previously been shown to have excellent inter-rater and intra-rater reliability (intraclass correlation 0.97; (Holmefur et al., 2007)), and is sensitive to change due to intervention (Eliasson et al., 2005). An alternate form of the AHA was used for adolescents older than 12 years provided by the developers, however its reliability has not yet been assessed. A certified rater scored the AHA. Raw AHA scores are based on 22 items scored from 1 to 4; hence raw AHA scores range from 22 to 88. Raw AHA scores were converted to scaled logit (log odds probability units) AHA scores, which range from 0 to 100 (Krumlinde-Sundholm, 2012).

2.3. MRI

To prepare children for the MRI scan, a "practice session" with a mock scanner was organised prior to the real MRI scan to familiarise children with the scanner conditions.

MRI data were acquired using a 3 T Siemens Tim Trio scanner (Siemens, Erlangen, Germany) with TQ gradients (45 mT/m, slew rate 200 T/m/s), using a 12 element Tim head array. A high-resolution structural image was acquired using a 0.9 mm isotropic 3D T1 Magnetization Prepared Rapid Gradient Echo (MPRAGE) sequence. The imaging parameters were: field of view $23 \times 23 \times 17.3$ cm; TR/TE/TI 1900/2.32/900 ms; and flip angle 9°. The acquisition time for the MPRAGE was 4.5 min.

Diffusion images were acquired using a commercial single shot twice-refocussed echo planar multi-directional diffusion weighted sequence (SS-EPI; Reese et al., 2003). The imaging parameters were: 60 axial slices; 2.5 mm slice thickness; field of view 30×30 cm; TR/TE 9500/116 ms; and acquisition matrix 128×128, resulting in an in-plane resolution of 2.34×2.34 mm. Parallel imaging was employed with an acceleration factor of 2 to reduce susceptibility distortions. Sixty-four diffusion weighted images were acquired at $b = 3000$ s/mm^2, in which the encoding gradients were distributed in space using the electrostatic approach (Jones et al., 1999), along with one minimally diffusion weighted image ($b = 0$). A field map for diffusion data was acquired using two 2D gradient-recalled echo images (36 axial slices; 3 mm slice thickness with 0.75 mm gap; field of view 19.2×19.2 cm; TR/TE1/TE2 488/4.92/7.38 ms; acquisition matrix 64×64) to assist in the correction for residual distortions due to susceptibility inhomogeneities. The combined acquisition time for diffusion data and field map was 10 min.

A Fluid Attenuated Inversion Recovery (FLAIR) image was acquired for lesion classification (25 axial slices; 4 mm slice thickness with 1.2 mm gap; field of view 22×22 cm; TR/TE/TI 7000/79/2500 ms; acquisition matrix 256×192 interpolated to 512×512). The acquisition time for the FLAIR image was 2 min.

Table 1
Demographics.

	CTD	Left hemiplegia	Right hemiplegia	p-Value	Left hemiplegia		Right hemiplegia		p-Value
		All lesions	All lesions		Unilateral lesion	Bilateral lesion	Unilateral lesion	Bilateral lesion	
Age	n = 17	n = 23	n = 27	0.530	n = 12	n = 11	n = 19	n = 8	0.292
Mean (SD)	11.3 (2.7)	10.5 (3)	11.4 (3.3)		9.4 (2.7)	11.7 (2.9)	11.6 (3.4)	10.9 (3)	
Range	7.7–16.3	5.1–17	6–17.1		5.5–14.2	5.1–17	6–17.1	6.3–14.9	
Gender	6/11	11/12	15/12		5/7	6/5	11/8	4/4	
MACS	N/A	I = 14	I = 11	0.162	I = 7	I = 7	I = 8	I = 3	0.568
		II = 9	II = 16		II = 5	II = 4	II = 11	II = 5	
GMFCS	N/A	I = 17	I = 13	0.063	I = 7	I = 10	I = 9	I = 4	0.115
		II = 6	II = 14		II = 5	II = 1	II = 10	II = 4	
AHA (scaled logit)	N/A	n = 21	n = 27	**0.021**	n = 12	n = 9	n = 19	n = 8	**0.011**
Mean (SD)		74 (13)	65 (13)		72 (13)	78 (12)	62 (10)	74 (15)	
Range		55–93	46–90		55–93	58–93	46–84	48–90	

CTD: children with typical development; MACS: Manual Ability Classification System; GMFCS: Gross Motor Function Classification System; AHA: Assisting Hand Assessment; logit: log-odds probability units; SD: standard deviation.
p-values smaller than 0.05 are highlighted in bold font.

2.4. Structural parcellation

Cortical reconstruction and volumetric segmentation were performed using the MPRAGE images with the Freesurfer image analysis suite (http://surfer.nmr.mgh.harvard.edu). Briefly, non-brain tissue was removed using a hybrid watershed/surface deformation procedure (Ségonne et al., 2004), subcortical white matter and deep grey matter volumetric structures were segmented automatically (Fischl et al., 2002, 2004b), and intensity inhomogeneity of the images was corrected (Sled et al., 1998). The cerebral cortex was parcellated into 34 units per hemisphere based on gyral and sulcal structures (Desikan et al., 2006; Fischl et al., 2004a). In addition to cortical regions, the left and right thalami, left and right cerebella, and brain stem were extracted. The accuracy of the cortical and subcortical parcellation was assessed visually. An axial slice was manually defined below the inferiormost slice on which the pons was visible to include only the most caudal part of the brain stem. Extracted cortical, subcortical and cerebellar structures are shown in Fig. 1.

A termination mask was generated to prevent diffusion tractography streamlines from crossing the cortical folds as described previously (Pannek et al., 2010). Briefly, the interface between WM and GM was identified, and this boundary shifted 1 voxel into the GM. Streamlines were terminated when penetrating more than 1 voxel deep into GM.

2.5. Diffusion processing

An extensive preprocessing procedure was followed to detect and correct for image artefacts caused by involuntary head motion, cardiac pulsation, and image distortions (Pannek et al., 2012a). In brief, image volumes with within-volume movement were detected using the discontinuity index (Nam and Park, 2011) and excluded from further analysis. Image distortions caused by susceptibility inhomogeneities were reduced using the field map, employing the FUGUE and PRELUDE tools available with FSL (Jenkinson et al., 2012), and intensity inhomogeneities were removed using n3 correction (Sled et al., 1998). Subsequently, signal intensity outlier voxels (caused by cardiac pulsation, bulk head motion and other artefacts) were detected and replaced using DROP-R (Morris et al., 2011). DROP-R was modified from the originally proposed method to employ a higher order model of the diffusion signal suitable for the detection and replacement of outliers in high b-value diffusion data (HOMOR, (Pannek et al., 2012b)). Between-volume registration to account for head movement during the scan time was performed using FMAM (Bai and Alexander, 2008) with adjustment of the b-matrix (Leemans and Jones, 2009; Rohde et al., 2004).

Following these steps, FA was estimated from the corrected diffusion data. Constrained spherical deconvolution (Tournier et al., 2007, 2012) (http://nitrc.org/projects/mrtrix) was employed to estimate the fibre orientation distribution for tractography at a maximum harmonic order of 8.

2.6. Connectome construction

Diffusion and structural data were co-registered using a rigid-body transformation with FLIRT (part of FSL; (Jenkinson et al., 2012)) by registering the FA to the skull-stripped MPRAGE. Registration accuracy was checked visually. Five million probabilistic streamlines were generated, seeding throughout the entire brain volume, to produce a whole brain tractogram. Streamlines were prevented from crossing cortical folds by applying the termination mask generated from structural data (see section Structural parcellation). Cortico-cortical, cortico-thalamic, cortico-cerebellar, and cerebello-cerebellar connections were extracted
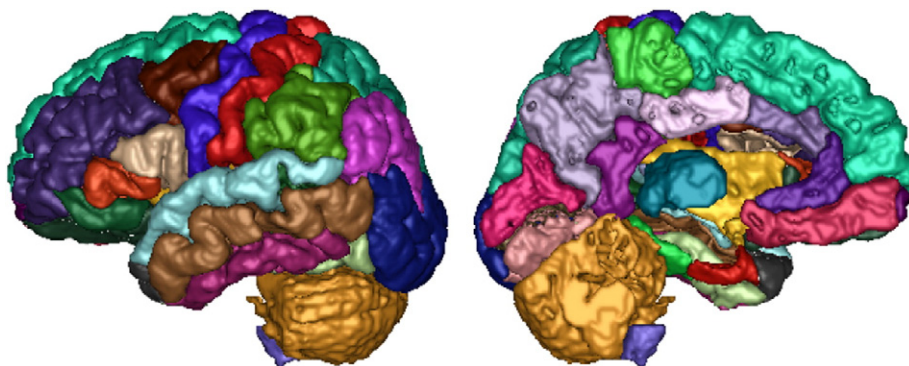
Fig. 1. Target regions used in the network analysis. Thirty-four cortical regions per hemisphere, the bilateral thalami, bilateral cerebella and brain stem were automatically delineated from high-resolution structural images using Freesurfer.

from the whole brain tractogram by hit-testing both terminal end points of every streamline with every cortical and cerebellar region. For brain stem connections, only one terminal endpoint was required to reside within the cortical, thalamic or cerebellar region, with any part of the streamline passing through the brain stem.

For every possible link between any pair of nodes, the number of connecting streamlines was noted. Median FA values were calculated by sampling the diffusion maps at every step of the selected streamlines. Connections with fewer than 250 streamlines (average) in children with typical development were excluded from further analysis (threshold determined empirically). Results were recorded in enriched connectivity matrices.

2.7. Lesion classification

A child neurologist expert in neuroimaging, who was blinded to clinical data, classified brain lesions based on structural images (MPRAGE and FLAIR) according to the presumed timing of lesion (Krägeloh-Mann and Horber, 2007). Each MRI was classified as: i) brain maldevelopments (BM), ii) periventricular white matter (PWM) lesions, iii) cortical or deep grey matter (CDGM) lesions or iv) miscellaneous (M). Additional information was recorded on location (lobes) and laterality of lesions. A semi-quantitative scale was used to systematically assess lesion severity on structural brain MRI (Fiori et al., 2014). Only children with PWM lesions were included in the final analysis; children with CDGM lesions were excluded due to failure of cortical parcellation, while children with brain maldevelopments were excluded due to the small group size (see also Subsection 3.1).

2.8. Statistical analysis

Statistical analysis of the brain network was performed using the NBS toolbox for Matlab (https://sites.google.com/site/bctnet/comparison/nbs; (Zalesky et al., 2010)). A general linear model was used to identify differences in FA between participant groups for every connection, using age as a confounding variable. The following comparisons were conducted:

1. CTD versus children with *left* unilateral CP caused PWM lesions;
2. CTD versus children with *right* unilateral CP caused by PWM lesions.

We hypothesised that FA would be reduced in children with unilateral CP compared to CTD, reflecting impaired WM organisation due to the brain lesion; and that there would be no increase in FA in children with unilateral CP compared to CTD.

In a subgroup analysis, we further investigated:

3. CTD versus children with *left* unilateral CP caused by *unilateral* PWM lesions;
4. CTD versus children with *left* unilateral CP caused by *bilateral* PWM lesions;
5. CTD versus children with *right* unilateral CP caused by *unilateral* PWM lesions;
6. CTD versus children with *right* unilateral CP caused by *bilateral* PWM lesions.

We hypothesised that an increased number of brain connections would exhibit alterations in FA in children with bilateral PWM lesions, primarily in interhemispheric connections and connections of the ipsilateral hemisphere. We further hypothesised that, in children with unilateral PWM lesions, alteration in FA would be restricted to the ipsilesional brain hemisphere, and interhemispheric motor connections.

A t-threshold of 3 was used for individual connections. Correction for multiple comparisons was performed using the network based statistic (NBS; (Zalesky et al., 2010)). The NBS identifies statistically significant components (i.e. "clusters" of connections), and can be thought of as the network analogue of conventional cluster statistics that is typically performed on statistical parametric maps. The NBS has a greater power than other correction methods such as Bonferroni correction or false discovery rate because it takes into account the interconnections (i.e. common nodes) between individual connections (Zalesky et al., 2010).

For connections that showed significant alterations in FA in children with unilateral CP compared to children with typical development, we additionally assessed the relationship between FA and clinical function (AHA) using a linear model. Statistical analyses were performed using R (R Development CoreTeam, 2008).
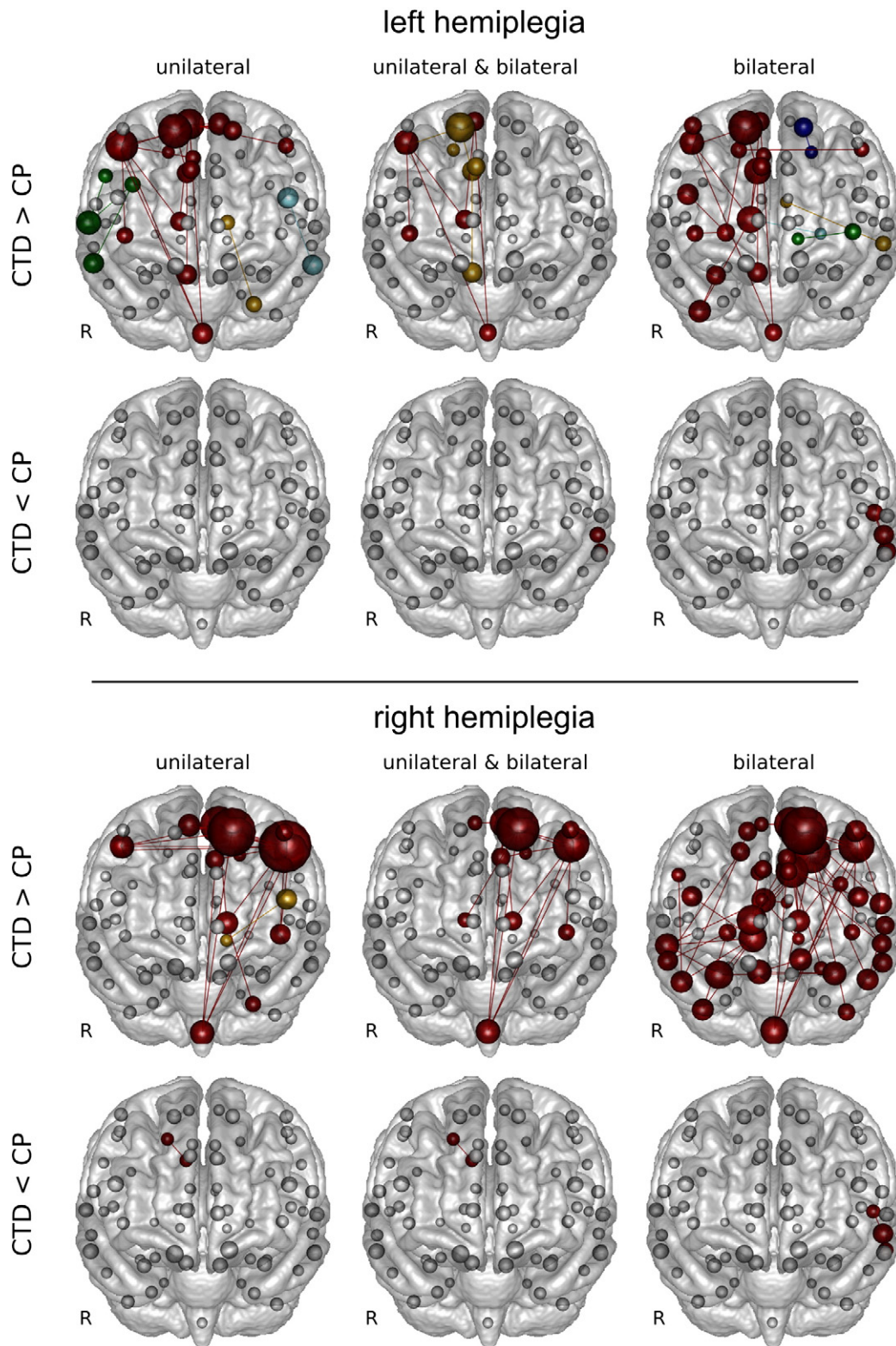
3. Results

3.1. Demographics

A total of 80 children with unilateral CP (38 children with left unilateral CP, and 42 children with right unilateral CP) and 21 children with typical development were recruited in this study. Automated cortical parcellation with Freesurfer failed frequently for children with CDGM lesions due to the size and extent of the lesion; example structural images are shown in Supplementary Fig. 1. Therefore, data of all 23 children with CDGM were excluded from further analysis (11 children with left unilateral CP and 12 children with right unilateral CP). Two children presented with brain malformation (1 left unilateral CP, and 1 right unilateral CP). Their data were also excluded due to the small sample size, resulting in a cohort of 55 children with PWM lesions (26 children with left unilateral CP and 29 children with right unilateral CP).

Data of 3 children with typical development and 5 children with PWM lesions (3 children with left unilateral CP and 2 children with right unilateral CP) were excluded due to excessive head movement artefacts or signal-to-noise problems on the MRIs.

The final cohort for analysis therefore consisted of 17 children with typical development (6 male, age range 7.7–16.3 years, mean age 11.3 [standard deviation 2.7] years), 23 children with left unilateral CP (11 male, age range 5.1–17.0 years, mean age 10.5 [standard deviation 3.0] years, MACS I = 14/II = 9, GMFCS I = 17/II = 6), and 27 children with right unilateral CP (15 male, age range 6.0–17.1 years, mean age 11.4 [standard deviation 3.3] years, MACS I = 11/II = 16, GMFCS I = 13/II = 14). Children with left unilateral CP included 11 children with unilateral PWM lesions and 12 children with bilateral PWM lesions, while children with right unilateral CP included 19 children with unilateral PWM lesions and 8 children with bilateral PWM lesions. For brevity, we refer to the brain hemisphere contralateral to the impaired limb as the "ipsilesional" hemisphere throughout the remainder of this manuscript.

Demographic information and lesion characteristics of included participants are summarised in Tables 1 and 2, respectively.

There was no difference in the means for age between CTD and children with left or right unilateral CP (ANOVA, p = 0.53), or for MACS and GMFCS between children with left or right unilateral CP (t-test, p = 0.16 and p = 0.06, respectively). Scaled logit AHA scores of children with right unilateral CP were significantly lower than scores of children with left unilateral CP (t-test, p = 0.021). There was a significant difference in scaled logit AHA mean scores between PWM lesion subgroups (ANOVA, p = 0.01). Post hoc analysis revealed that scaled logit AHA scores of children with left unilateral CP caused by unilateral PWM lesions were higher than scores of children with right unilateral CP caused by unilateral PWM lesions (p = 0.047, t-test); and scaled logit AHA scores of children with left unilateral CP caused by bilateral PWM lesions were higher than scores of children with right unilateral CP caused by unilateral PWM lesions (p = 0.004, t-test). There were no differences in age, MACS or GMFCS between PWM lesion subgroups (ANOVA). There were no differences in hemispheric, hemispheric summary (including the basal ganglia, brainstem, thalamus and posterior limb of the internal capsule ipsilaterally), basal ganglia & brainstem (including the thalamus, and posterior limb of the internal capsule bilaterally) and global (including the corpus callosum and cerebellum bilaterally) scores between the left and right hemiplegia groups (t-tests).

Fig. 2. Results of the network-based statistic analysis (NBS). Alterations in fractional anisotropy (FA) compared to children with typical development were detected in children with left unilateral CP (top) and children with right unilateral CP (bottom). Results are shown for the comparison between children with typical development (CTD) and children with unilateral PWM lesions (left); between CTD and children with bilateral PWM lesions (right); and between CTD and the combined cohort of children with PWM lesions (i.e. the combined unilateral and bilateral cohorts; middle). Node colour indicates network membership. The size of the nodes indicates the number of connections of this node exhibiting reduced FA.

3.2. Alterations in FA in children with unilateral CP

A total of 557 connections with an average of more than 250 streamlines in children with typical development were assessed. Results of the NBS analysis are summarised in Fig. 2. All connections that were identified as having significantly altered FA in children with unilateral CP compared to children with typical development are listed in Tables 3 and 4, along with mean FA values for those connections.

Table 2
Lesion scores.

	Left hemiplegia			Right hemiplegia		
	All lesions	Unilateral lesions	Bilateral lesions	All lesions	Unilateral lesions	Bilateral lesions
Global mean (SD)	7.22 (4.88)	4.71 (1.56)	9.95 (5.83)	8.81 (2.82)	6.26 (2.32)	8.12 (3.58)
Hemispheric R mean (SD)	3.61 (1.74)	2.96 (0.84)	4.32 (2.21)	1.02 (1.79)	0.16 (0.69)	3.06 (1.97)
Hemispheric L mean (SD)	1.52 (2.05)	0.00 (0.00)	3.18 (1.86)	3.06 (1.33)	2.79 (1.03)	3.69 (1.79)
Summary R mean (SD)	5.09 (2.72)	4.54 (1.68)	5.68 (3.52)	1.02 (1.79)	0.16 (0.69)	3.06 (1.97)
Summary L mean (SD)	1.52 (2.05)	0.00 (0.00)	3.18 (1.86)	5.31 (1.87)	5.58 (1.95)	4.69 (1.58)
BG & BS mean (SD)	1.48 (1.62)	1.58 (1.62)	1.36 (1.69)	2.26 (1.51)	2.79 (1.32)	1.00 (1.20)

R—right; L—left; BG—basal ganglia; BS—brain stem.

3.2.1. Alterations in FA in children with left unilateral CP

FA was reduced in two network components. Component 1 comprised 5 ipsilesional intrahemispheric connections between 5 nodes (p = 0.003), and included right motor corticospinal connections (between the brain stem and pre- and paracentral gyri); right motor thalamocortical connections (between the thalamus and pre- and paracentral gyri), and the connection between the right precentral gyrus and the right insular cortex. Component 2 comprised 5 ipsilesional intrahemispheric fronto-parietal connections between 6 nodes (p = 0.004). Component 2 included the connections between the right precuneus and right medial orbitofrontal lobe, right caudal anterior cingulate, and right superior frontal lobes; further, it included the connections between the right superior frontal lobe and right postcentral, and right superior parietal cortex. FA was increased in children with left unilateral CP in a network component comprising 1 contralesional intrahemispheric connection between 2 nodes (p = 0.018): the connection between left middle temporal and superior temporal gyri.

3.2.2. Alterations in FA in children with right unilateral CP

FA was reduced in a network component comprising 16 connections between 12 nodes (p = 0.004). This network included left corticospinal connections (between the brain stem and left precentral, postcentral, paracentral and superior frontal lobes); left thalamocortical connections (between the thalamus and paracentral and precentral gyri); association connections of the left superior frontal lobe and left precentral, postcentral, and paracentral superior parietal lobes, and right thalamus; the connection between the left precentral gyrus and insular cortex; the connection between the left posterior cingulate and left pre- and paracentral gyri; and interhemispheric connection between left and right paracentral cortices. FA was increased in children with right

unilateral CP in a network component comprising 1 contralesional intrahemispheric connection between 2 nodes (p = 0.018): right precuneus and superior parietal lobe.

3.2.3. Similarities between unilateral CP groups

A total of 7 connections were identified simultaneously for children with left and right unilateral CP when the side of the primary lesion was used as a reference point: corticospinal connections (between the brain stem and precentral and paracentral gyri); motor thalamocortical connections (between the thalamus and precentral and paracentral gyri); and association connections between the postcentral gyrus and superior frontal lobe; precentral gyrus and insular cortex; and superior frontal lobe and superior parietal lobe. These connections were used to investigate the relationship between microstructure (i.e. FA) and clinical function (AHA).

3.3. Alterations in FA in children with unilateral and bilateral PWM lesions

Children with unilateral CP due to PWM damage can present with unilateral or bilateral lesions. In a subanalysis, we explored whether different brain networks were altered in children with unilateral or bilateral brain lesions. Results are presented in Fig. 2.

All groups showed reductions in FA in corticospinal and thalamocortical connections, as well as in fronto-parietal association pathways. An increased number of interhemispheric connections showed reductions in FA compared to the assessment of the mixed cohort. Children with bilateral brain lesions also showed reduced FA in connections of the hemisphere ipsilateral to the impaired hand (i.e. "contra-lesional" hemisphere). Children with right unilateral CP caused by bilateral PWM lesions showed widespread reductions in FA.

A small number of connections showed increased FA compared to CTD: in children with bilateral PWM lesions (both with left and with right unilateral CP), FA was increased in a small network of left temporal regions; in children with right unilateral CP caused by a unilateral brain lesion, FA was increased in the connection between the right superior parietal lobe and right precuneus.

3.4. Relationship between FA and AHA score

A positive relationship between FA and AHA scores, indicating an association between better WM microstructural organisation and better performance of the impaired hand in bimanual tasks, was found in 6 of the 7 assessed connections for children with left unilateral CP (p < 0.05, r^2 = 0.22–0.44). There was a moderate relationship between AHA and FA of the connection between brain stem and right precentral gyrus (r^2 = 0.44); and a moderate relationship between AHA and FA of the connection between the right thalamus and right paracentral gyrus (r^2 = 0.37), the connection between the right postcentral gyrus and right superior frontal lobe (r^2 = 0.35), the connection between the

Table 3
Results of FA comparison for left hemiplegia group.

Connection	CTD	Left hemiplegia	t-Stat
Brain stem–right paracentral	0.46 (0.02)	0.42 (0.02)	5.80
Brain stem–right precentral	0.45 (0.03)	0.41 (0.03)	4.80
Right thalamus–right paracentral	0.44 (0.03)	0.38 (0.03)	6.49
Right thalamus–right precentral	0.44 (0.03)	0.40 (0.03)	4.98
Right precentral–right insula	0.36 (0.02)	0.33 (0.02)	3.99
Right precuneus–right medial orbito-frontal	0.35 (0.03)	0.32 (0.03)	3.64
Right precuneus–right caudal anterior cingulate	0.32 (0.03)	0.29 (0.03)	3.92
Right precuneus–right superior frontal	0.37 (0.03)	0.34 (0.03)	3.50
Right superior frontal–right postcentral	0.37 (0.02)	0.35 (0.02)	4.94
Right superior frontal–right superior parietal	0.41 (0.03)	0.37 (0.03)	4.29
Left middle temporal–left superior temporal	0.28 (0.02)	0.30 (0.02)	−3.21

Reported values are mean (standard deviation) of fractional anisotropy; CTD: children with typical development.

Table 4
Results of FA comparison for right hemiplegia group.

Connection	CTD	Right hemiplegia	t-Stat
Brain stem–left superior frontal	0.41 (0.03)	0.39 (0.03)	3.67
Brain stem–left precentral	0.45 (0.03)	0.39 (0.04)	7.01
Brain stem–left postcentral	0.44 (0.04)	0.40 (0.04)	4.10
Brain stem–left paracentral	0.46 (0.04)	0.40 (0.04)	5.29
Left thalamus–left paracentral	0.44 (0.05)	0.36 (0.05)	6.09
Left thalamus–left precentral	0.45 (0.05)	0.36 (0.05)	6.87
Right thalamus–left superior frontal	0.44 (0.04)	0.41 (0.04)	3.39
Left superior frontal–left paracentral	0.30 (0.04)	0.26 (0.04)	4.49
Left superior frontal–left postcentral	0.37 (0.04)	0.34 (0.04)	3.56
Left superior frontal–left precentral	0.38 (0.05)	0.33 (0.05)	3.43
Left superior frontal–left superior parietal	0.41 (0.03)	0.38 (0.03)	3.88
Left precentral–left insula	0.36 (0.04)	0.32 (0.03)	5.58
Left precentral–left posterior cingulate	0.43 (0.05)	0.35 (0.05)	4.39
Left caudal middle frontal–left precentral	0.33 (0.04)	0.30 (0.04)	3.30
Left paracentral–left posterior cingulate	0.37 (0.06)	0.31 (0.06)	3.83
Left paracentral–right paracentral	0.48 (0.07)	0.40 (0.07)	4.18
Right precuneus–right superior parietal	0.24 (0.03)	0.26 (0.03)	−3.21

Reported values are mean (standard deviation) of fractional anisotropy; CTD: children with typical development.

Table 5
Association between AHA and FA.

Connection	Left hemiplegia	Right hemiplegia
Brain stem–precentral	$r^2 = 0.44$ (p = 0.001)	$r^2 = 0.33$ (p = 0.002)
Brain stem–paracentral	$r^2 = 0.29$ (p = 0.011)	$r^2 = 0.16$ (p = 0.036)
Thalamus–precentral	$r^2 = 0.24$ (p = 0.025)	$r^2 = 0.36$ (p = 0.001)
Thalamus–paracentral	$r^2 = 0.37$ (p = 0.003)	$r^2 = 0.19$ (p = 0.021)
Postcentral–superior frontal	$r^2 = 0.35$ (p = 0.005)	$r^2 = 0.22$ (p = 0.013)
Precentral–insula	$r^2 = 0.22$ (p = 0.032)	$r^2 = 0.14$ (p = 0.052)
Superior frontal–superior parietal	$r^2 = 0.002$ (p = 0.57)	$r^2 = 0.03$ (p = 0.39)

AHA: Assisting Hand Assessment; FA: fractional anisotropy.

brain stem and right paracentral gyrus ($r^2 = 0.29$), the connection between the right thalamus and right precentral gyrus ($r^2 = 0.24$), and the connection between the right precentral gyrus and insular cortex ($r^2 = 0.22$). There was no relationship between AHA and FA of the connection between the superior frontal and superior parietal lobes (p = 0.568, $r^2 = 0.02$).

For children with left unilateral CP, a positive relationship between AHA and FA was found for 5 of the 7 assessed connections (p < 0.05; $r^2 = 0.16$–0.36). We found a moderate relationship between AHA and FA of the connection between the left thalamus and left precentral gyrus ($r^2 = 0.36$), the connection between the brain stem and left precentral gyrus ($r^2 = 0.33$), the connection between the left postcentral gyrus and left superior frontal lobe ($r^2 = 0.22$), and the connection between the left thalamus and left paracentral lobe ($r^2 = 0.21$). There was a weak association between AHA and FA of the connection between the brain stem and left paracentral gyrus ($r^2 = 0.16$). The weak relationship between AHA and FA of the connection between the precentral and insular regions approached, but did not reach, significance (p = 0.052; $r^2 = 0.14$). There was no relationship between AHA and FA of the connection between the superior frontal and superior parietal lobes (p = 0.39; $r^2 = 0.03$). Results of the correlation analysis are summarised in Table 5, and graphically displayed in Supplementary Fig. 2.

4. Discussion

This study is the first to employ a network-based statistical (NBS) analysis of the structural connectome, using combined high-resolution structural imaging and probabilistic tractography incorporating crossing fibres, to identify connections of altered diffusion in children with unilateral CP compared to children with typical development. In children with unilateral CP, FA was reduced in a number of ipsilesional cortico-cortical, ipsilesional thalamocortical and ipsilesional corticospinal tracts. Connections of the pre-, post- and paracentral gyri, the superior frontal lobe, the superior parietal lobe and the precuneus were frequently identified. Seven connections, including corticospinal, thalamocortical, fronto-parietal, and precentral–insular tracts, were identified simultaneously in children with left and right unilateral CP when the side of lesion was used as a reference point. Additionally, relationships between WM microstructure (FA) and clinical function (performance of the impaired hand in bimanual tasks) were evidenced in the majority of these connections (Table 5).

The analyses performed here confirm alterations in connectivity of several motor pathways described previously (Scheck et al., 2012), including the corticospinal tract, thalamocortical connections, and fronto-parietal pathways. One of the advantages of using the network-

based technique employed here is, however, that no a priori hypothesis regarding the impacted pathways is required. A number of pathways that have not previously been studied in the context of unilateral cerebral palsy could therefore be identified. These connections include motor connections to the insula and the anterior cingulate gyrus. Application of this technique to investigate alterations in connectivity following treatment may elucidate the neurological correlates of improved functioning due to intervention. In addition, connectivity differences between children with different responses to treatment may aid in the selection of interventions for the individual patient.

The techniques used here are, in contrast to those employed in many other tractography studies, fully automated. Cortical and subcortical regions are automatically identified from the structural image, and are applied to identify pathways from whole brain tractograms. The cortical and subcortical parcellation is based on the anatomy of the individual participant, and it has been shown that the accuracy of this automated parcellation approximates that of manual parcellation (Desikan et al., 2006). With the use of an individualised parcellation, only rigid alignment of diffusion and structural images is required as opposed to non-linear registration to a template (which would be required for atlas based parcellation). Non-linear registration can be particularly challenging in the presence of large lesions or significantly enlarged ventricles that are often seen in children with CP. A limitation of the parcellation based on individual anatomy is, however, that the cerebral cortex cannot be correctly segmented in the presence of large cortical lesions. This is of particular relevance as to the generalizability of our results. Indeed, automated cortical parcellation failed in the majority of subjects with CDGM lesions; subsequently, all subjects with CDGM lesions were excluded from this analysis, providing a clean cohort of children with PWM lesions. Our analysis can therefore only be considered relevant for this form of congenital brain lesion. In addition, children included in this study had mild to moderate CP (GMFCS I–II, MACS I–II); hence our results cannot be generalized to more severe CP.

A rigorous preprocessing pipeline (Pannek et al., 2012a,b) ensures adequate data quality by identifying and removing artefacts caused by involuntary head movement and cardiac pulsation; correction for distortions caused by susceptibility inhomogeneities improves the co-registration of diffusion and structural images; and the use of a higher order model of the diffusion signal enables the resolution of crossing fibres in complex white matter architecture, which has been shown to significantly improve the accuracy of tractography (Jones, 2008). Pathways of altered connectivity could be identified using the recently introduced network based statistic (Zalesky et al., 2010). Furthermore, our analysis included not only cortical regions, but also the cerebellum, thalamus and brainstem—regions that are often neglected in connectome analysis, but play a crucial role in elucidating the brain injury in cerebral palsy. Connectivity of pathways was assessed using FA rather than streamline number or tract volume because of problems in normalisation (e.g. differences in brain size and shape) and interpretation (Jones et al., 2012). A summary measure of FA within connections is, on the other hand, directly comparable across participants. While FA is highly sensitive to microstructural changes, it is not specific to the type of change (myelination, axon density, axon coherence, maturation/degeneration; Alexander et al., 2011).

It should be noted, however, that in regions of crossing fibres, counterintuitive changes in FA (and other diffusion tensor-based metrics) can be observed when only one fibre population is affected (Wheeler-Kingshott and Cercignani, 2009). In crossing fibre regions, anisotropy measured using the diffusion tensor may be low despite high coherence within the individual fibre bundles—a direct consequence of the tensor's inability to resolve crossing fibres. If the microstructural organisation of one fibre bundle is reduced due to pathology, (tensor) anisotropy may be artefactually increased. In this study, we identified a small network of connections that showed increased FA in children with bilateral PWM lesions was located within the temporal lobe—a region of highly complex white matter architecture. We therefore speculate that the finding of increased FA in children with bilateral PWM lesions is artefactual rather than representing a compensatory mechanism in response to brain injury. The use of novel, quantitative diffusion metrics, such as the recently proposed apparent fibre density (Raffelt et al., 2012), may be more suited to detecting alterations in microstructure in these highly complex areas.

With the whole-brain approach employed here, we identified pathways known to be impacted by brain lesions in unilateral CP, including the ipsilesional descending motor cortico-spinal tract and the ipsilesional ascending motor thalamo-cortical tract. These pathways are thought to be the main contributors to the motor impairments seen in children with CP (Rose et al., 2011). The superior longitudinal fasciculus (identified here as fronto-parietal connections) has also previously been shown to be altered in children with spastic CP (Yoshida et al., 2011), however no involvement of the superior longitudinal fasciculus was found in another study of children with unilateral CP (Thomas et al., 2005). The fronto-parietal part of the superior longitudinal fasciculus is thought to be involved in regulating the higher aspects of motor behaviour (Makris et al., 2005).

In addition to these pathways which are known to be impacted by brain lesions in CP, we also identified connections of the insula and the anterior and posterior cingulate gyri. The insular cortex and posterior cingulate gyrus are non-primary motor areas (Fink et al., 1997), and involvement of their connections may contribute to the impairments seen in CP. The insula and anterior cingulate cortex have been linked to implicit motor awareness in adults with acquired hemiparesis (Moro et al., 2011), resulting in possible implications for rehabilitation. The posterior cingulate cortex is involved in visuo-spatial processing and it demonstrated connections to numerous premotor areas including the cingulate motor areas (Vogt et al., 2006), suggesting a possible role in orientation of self and body in visual space in hemiplegic subjects.

It should be noted that while we identified alterations in FA of connections between the thalamus and the precentral and paracentral gyri, respectively, between CP and CTD groups, we found no difference in FA of the connection between the thalamus and the postcentral gyrus. Our previous research, which involved an overlapping (Tsao et al., 2013) and an independent cohort (Rose et al., 2011), revealed an ipsilesional–contralesional asymmetry in these thalamo-sensory fibres (measured by streamline number and FA), which also correlated with hand function of the paretic hand. The current study did not assess hemispheric asymmetry of connections, but rather identified differences between patient and control groups, and did not reveal any difference in FA for the thalamo-sensory pathway.

Our assessment of the relationship between clinical function and microstructure in pathways impacted by brain lesions in CP showed that microstructural alterations of the cortico-spinal and thalamo-cortical pathways were significantly associated with deficits in performance of the impaired hand in bimanual tasks (measured using AHA). As mentioned above, it is important to recognize that this finding in children with PWM lesions is not necessarily generalizable to other types of brain lesions observed in CP (e.g. CDGM lesion or brain malformation).

Our subanalysis of children with unilateral or bilateral PWM lesions as separate group, revealed that, in general, the same connections were identified when unilateral CP groups were assessed by lesion group

compared to a mixed-lesion cohort: motor connections of the brain stem and thalamus, as well as fronto-parietal connections showed reduced FA in all cases. A larger number of interhemispheric connections, and contralesional interhemispheric connections were identified for both the unilateral and bilateral lesion groups than were identified when assessing a mixed cohort. Children with right unilateral CP and bilateral lesions showed widespread alterations in FA compared to CTD that were not observed in the children with left unilateral CP or children with light unilateral CP caused by unilateral PWM lesions. Whether these widespread alterations represent a true finding, or are an artefact caused by small participant numbers (n = 8) is unclear. A larger cohort of children with unilateral CP will be required for this analysis.

5. Conclusion

In conclusion, we identified pathways of altered structural connectivity in children with unilateral CP compared to children with typical development. Our analysis revealed that impacted connections include ipsilesional projection and association pathways. Several pathways that have not previously been studied in CP also showed alterations in microstructure both in children with left, and in children with right unilateral CP. Relationships between white matter microstructure and clinical function were found within these connections. Subgroup analysis, separating unilateral and bilateral lesions during statistical analysis, revealed that, while the microstructure of corticospinal, cortico-thalamic, and fronto-parietal connections is altered in all cases, interhemispheric and ipsilateral connections may be impacted differently.

Supplementary data to this article can be found online at http://dx.doi.org/10.1016/j.nicl.2014.05.018.

References

Alexander, A.L., Hurley, S.A., Samsonov, A.A., Adluru, N., Hosseinbor, A.P., Mossahebi, P., Field, A.S., 2011. Characterization of cerebral white matter properties using quantitative magnetic resonance imaging stains. Brain Connect. 1 (6), 423–446. http://dx.doi.org/10.1089/brain.2011.007.

Arnfield, E., Guzzetta, A., Boyd, R., 2013. Relationship between brain structure on magnetic resonance imaging and motor outcomes in children with cerebral palsy: a systematic review. Res. Dev. Disabil. 34 (7), 2234–2250. http://dx.doi.org/10.1016/j.ridd.2013.03.031.

Bai, Y., Alexander, D.C., 2008. Model-based registration to correct for motion between acquisitions in diffusion MR imaging. Biomedical Imaging: From Nano to Macro, 2008. ISBI 2008. 5th IEEE International Symposium on, pp. 947–950.

Basser, P.J., Ozarslan, E., 2010. Anisotropic diffusion: from the apparent diffusion coefficient to the apparent diffusion tensor. In: Jones, D.K. (Ed.), Diffusion MRI: Theory, Methods, and Applications. Oxford University Press, pp. 79–91.

Bodimeade, H.L., Whittingham, K., Lloyd, O., Boyd, R.N., 2013. Executive functioning in children with unilateral cerebral palsy: protocol for a cross-sectional study. BMJ Open 3 (4). http://dx.doi.org/10.1136/bmjopen-2012-002500.

Boyd, R.N., Mitchell, L.E., James, S.T., Ziviani, J., Sakzewski, L., Smith, A., Scuffham, P.A., 2013a. Move it to improve it (Mitii): study protocol of a randomised controlled trial of a novel web-based multimodal training program for children and adolescents with cerebral palsy. BMJ Open 3 (4). http://dx.doi.org/10.1136/bmjopen-2013-002853.

Boyd, R.N., Ziviani, J., Sakzewski, L., Miller, L., Bowden, J., Cunnington, R., Rose, S., 2013b. COMBIT: protocol of a randomised comparison trial of combined modified constraint induced movement therapy and bimanual intensive training with distributed model of standard upper limb rehabilitation in children with congenital hemiplegia. BMC Neurol. 13, 68. http://dx.doi.org/10.1186/1471-2377-13-68.

Chang, M.C., Jang, S.H., Yoe, S.S., Lee, E., Kim, S., Lee, D.G., Son, S.M., 2012. Diffusion tensor imaging demonstrated radiologic differences between diplegic and quadriplegic cerebral palsy. Neurosci. Lett. 512 (1), 53–58. http://dx.doi.org/10.1016/j.neulet.2012.01.065.

Chaturvedi, S.K., Rai, Y., Chourasia, A., Goel, P., Paliwal, V.K., Garg, R.K., Gupta, R.K., 2012. Comparative assessment of therapeutic response to physiotherapy with or without botulinum toxin injection using diffusion tensor tractography and clinical scores in term diplegic cerebral palsy children. Brain Dev. http://dx.doi.org/10.1016/j.braindev.2012.10.012.

Desikan, R.S., Ségonne, F., Fischl, B., Quinn, B.T., Dickerson, B.C., Blacker, D., Killiany, R.J., 2006. An automated labeling system for subdividing the human cerebral cortex on MRI scans into gyral based regions of interest. NeuroImage 31 (3), 968–980. http://dx.doi.org/10.1016/j.neuroimage.2006.01.021.

Eliasson, A.-C., Krumlinde-Sundholm, L., Shaw, K., Wang, C., 2005. Effects of constraint-induced movement therapy in young children with hemiplegic cerebral palsy: an adapted model. Dev. Med. Child Neurol. 47 (4), 266–275.

Fink, G.R., Frackowiak, R.S., Pietrzyk, U., Passingham, R.E., 1997. Multiple nonprimary motor areas in the human cortex. J. Neurophysiol. 77 (4), 2164–2174.

Fiori, S., Cioni, G., Klingels, K., Ortibus, E., Van Gestel, L., Rose, S., Guzzetta, A., 2014. Reliability of a novel, semi-quantitative scale for classification of structural brain magnetic resonance imaging in children with cerebral palsy. Dev. Med. Child Neurol. http://dx.doi.org/10.1111/dmcn.1245.

Fischl, B., Salat, D.H., Busa, E., Albert, M., Dieterich, M., Haselgrove, C., Dale, A.M., 2002. Whole brain segmentation: automated labeling of neuroanatomical structures in the human brain. Neuron 33 (3), 341–355.

Fischl, B., Salat, D.H., van der Kouwe, A.J.W., Makris, N., Ségonne, F., Quinn, B.T., Dale, A.M., 2004a. Sequence-independent segmentation of magnetic resonance images. NeuroImage 23 (Suppl. 1), S69–S84. http://dx.doi.org/10.1016/j.neuroimage.2004.07.016.

Fischl, B., van der Kouwe, A., Destrieux, C., Halgren, E., Ségonne, F., Salat, D.H., Dale, A.M., 2004b. Automatically parcellating the human cerebral cortex. Cereb. Cortex 14 (1), 11–22.

Glenn, O.A., Ludeman, N.A., Berman, J.I., Wu, Y.W., Lu, Y., Bartha, A.I., Henry, R.G., 2007. Diffusion tensor MR imaging tractography of the pyramidal tracts correlates with clinical motor function in children with congenital hemiparesis. Am. J. Neuroradiol. 28 (9), 1796–1802. http://dx.doi.org/10.3174/ajnr.A0676.

Holmefur, M., Krumlinde-Sundholm, L., Eliasson, A.-C., 2007. Interrater and intrarater reliability of the assisting hand assessment. Am. J. Occup. Ther. 61 (1), 79–84.

Holmström, L., Lennartsson, F., Eliasson, A.-C., Flodmark, O., Clark, C., Tedroff, K., Vollmer, B., 2011. Diffusion MRI in corticofugal fibers correlates with hand function in unilateral cerebral palsy. Neurology 77 (8), 775–783. http://dx.doi.org/10.1212/WNL.0b013e31822b0040.

Hoon, A.H., Lawrie, W.T., Melhem, E.R., Reinhardt, E.M., Van Zijl, P.C.M., Solaiyappan, M., Mori, S., 2002. Diffusion tensor imaging of periventricular leukomalacia shows affected sensory cortex white matter pathways. Neurology 59 (5), 752–756.

Jenkinson, M., Beckmann, C.F., Behrens, T.E.J., Woolrich, M.W., Smith, S.M., 2012. FSL. NeuroImage 62 (2), 782–790. http://dx.doi.org/10.1016/j.neuroimage.2011.09.015.

Jones, D.K., 2008. Studying connections in the living human brain with diffusion MRI. Cortex 44 (8), 936–952. http://dx.doi.org/10.1016/j.cortex.2008.05.002.

Jones, D.K., Horsfield, M.A., Simmons, A., 1999. Optimal strategies for measuring diffusion in anisotropic systems by magnetic resonance imaging. Magn. Reson. Med. 42 (3), 515–525.

Jones, D.K., Knösche, T.R., Turner, R., 2012. White matter integrity, fiber count, and other fallacies: the do's and don'ts of diffusion MRI. NeuroImage. http://dx.doi.org/10.1016/j.neuroimage.2012.06.081.

Koerte, I., Pelavin, P., Kirmess, B., Fuchs, T., Berweck, S., Laubender, R.P., Heinen, F., 2011. Anisotropy of transcallosal motor fibres indicates functional impairment in children with periventricular leukomalacia. Dev. Med. Child Neurol. 53 (2), 179–186. http://dx.doi.org/10.1111/j.1469-8749.2010.03840.x.

Krägeloh-Mann, I., Horber, V., 2007. The role of magnetic resonance imaging in elucidating the pathogenesis of cerebral palsy: a systematic review. Dev. Med. Child Neurol. 49 (2), 144–151. http://dx.doi.org/10.1111/j.1469-8749.2007.00144.x.

Krumlinde-Sundholm, L., 2012. Reporting outcomes of the assisting hand assessment: what scale should be used? Dev. Med. Child Neurol. 54 (9), 807–808. http://dx.doi.org/10.1111/j.1469-8749.2012.04361.x.

Krumlinde-Sundholm, L., Eliasson, A.-C., 2003. Development of the assisting hand assessment: a Rasch-built measure intended for children with unilateral upper limb impairments. Scand. J. Occup. Ther. 10 (1), 16–26.

Leemans, A., Jones, D.K., 2009. The B-matrix must be rotated when correcting for subject motion in DTI data. Magn. Reson. Med. 61 (6), 1336–1349. http://dx.doi.org/10.1002/mrm.21890.

Makris, N., Kennedy, D.N., McInerney, S., Sorensen, A.G., Wang, R., Caviness, V.S., Pandya, D.N., 2005. Segmentation of subcomponents within the superior longitudinal fascicle in humans: a quantitative, in vivo, DT-MRI study. Cereb. Cortex 15 (6), 854–869. http://dx.doi.org/10.1093/cercor/bhh186.

Miller, F., 2005. Etiology, epidemiology, pathology, and diagnosis. Cerebral Palsy. Springer, New York, pp. 27–50.

Moro, V., Pernigo, S., Zapparoli, P., Cordioli, Z., Aglioti, S.M., 2011. Phenomenology and neural correlates of implicit and emergent motor awareness in patients with anosognosia for hemiplegia. Behav. Brain Res. 225 (1), 259–269. http://dx.doi.org/10.1016/j.bbr.2011.07.010.

Morris, D., Nossin-Manor, R., Taylor, M.J., Sled, J.G., 2011. Preterm neonatal diffusion processing using detection and replacement of outliers prior to resampling. Magn. Reson. Med. 66 (1), 92–101. http://dx.doi.org/10.1002/mrm.22786.

Nam, H., Park, H.-J., 2011. Distortion correction of high b-valued and high angular resolution diffusion images using iterative simulated images. NeuroImage 57 (3), 968–978. http://dx.doi.org/10.1016/j.neuroimage.2011.05.018.

Pannek, K., Mathias, J.L., Bigler, E.D., Brown, G., Taylor, J.D., Rose, S., 2010. An automated strategy for the delineation and parcellation of commissural pathways suitable for clinical populations utilising high angular resolution diffusion imaging tractography. NeuroImage 50 (3), 1044–1053. http://dx.doi.org/10.1016/j.neuroimage.2010.01.020.

Pannek, K., Guzzetta, A., Colditz, P.B., Rose, S.E., 2012a. Diffusion MRI of the neonate brain: acquisition, processing and analysis techniques. Pediatr. Radiol. 42 (10), 1169–1182. http://dx.doi.org/10.1007/s00247-012-2427-.

Pannek, K., Raffelt, D., Bell, C., Mathias, J.L., Rose, S.E., 2012b. HOMOR: higher order model outlier rejection for high b-value MR diffusion data. NeuroImage 63 (2), 835–842. http://dx.doi.org/10.1016/j.neuroimage.2012.07.022.

R Development CoreTeam, 2008. R: a Language and Environment for Statistical Computing. R Foundation Statistical Computing.

Raffelt, D., Tournier, J.D., Rose, S., Ridgway, G.R., Henderson, R., Crozier, S., Connelly, A., 2012. Apparent fibre density: a novel measure for the analysis of diffusion-weighted magnetic resonance images. NeuroImage 59 (4), 3976–3994. http://dx.doi.org/10.1016/j.neuroimage.2011.10.04.

Reese, T.G., Heid, O., Weisskoff, R.M., Wedeen, V.J., 2003. Reduction of eddy-current-induced distortion in diffusion MRI using a twice-refocused spin echo. Magn. Reson. Med. 49 (1), 177–182. http://dx.doi.org/10.1002/mrm.1030.

Rha, D.-W., Chang, W.H., Kim, J., Sim, E.G., Park, E.S., 2012. Comparing quantitative tractography metrics of motor and sensory pathways in children with periventricular leukomalacia and different levels of gross motor function. Neuroradiology 54 (6), 615–621. http://dx.doi.org/10.1007/s00234-011-0996-2.

Rohde, G.K., Barnett, A.S., Basser, P.J., Marenco, S., Pierpaoli, C., 2004. Comprehensive approach for correction of motion and distortion in diffusion-weighted MRI. Magn. Reson. Med. 51 (1), 103–114. http://dx.doi.org/10.1002/mrm.10677.

Rose, S., Guzzetta, A., Pannek, K., Boyd, R., 2011. MRI structural connectivity, disruption of primary sensorimotor pathways, and hand function in cerebral palsy. Brain Connect. 1 (4), 309–316. http://dx.doi.org/10.1089/brain.2011.0034.

Rosenbaum, P., Paneth, N., Leviton, A., Goldstein, M., Bax, M., Damiano, D., Jacobsson, B., 2007. A report: the definition and classification of cerebral palsy April 2006. Dev. Med. Child Neurol. Suppl. 109, 8–14.

Scheck, S.M., Boyd, R.N., Rose, S.E., 2012. New insights into the pathology of white matter tracts in cerebral palsy from diffusion magnetic resonance imaging: a systematic review. Dev. Med. Child Neurol. 54 (8), 684–696. http://dx.doi.org/10.1111/j.1469-8749.2012.04332.x.

Scholz, J., Tomassini, V., Johansen-Berg, H., 2009. Individual differences in white matter microstructure in the healthy brain. Diffusion MRI: From Quantitative Measurement to In-vivo Neuroanatomy, pp. 237–247.

Ségonne, F., Dale, A.M., Busa, E., Glessner, M., Salat, D., Hahn, H.K., Fischl, B., 2004. A hybrid approach to the skull stripping problem in MRI. NeuroImage 22 (3), 1060–1075. http://dx.doi.org/10.1016/j.neuroimage.2004.03.032.

Sled, J.G., Zijdenbos, A.P., Evans, A.C., 1998. A nonparametric method for automatic correction of intensity nonuniformity in MRI data. IEEE Trans. Med. Imaging 17 (1), 87–97. http://dx.doi.org/10.1109/42.668698.

Son, S.M., Ahn, Y.H., Sakong, J., Moon, H.K., Ahn, S.H., Lee, H., Jang, S.H., 2007. Diffusion tensor imaging demonstrates focal lesions of the corticospinal tract in hemiparetic patients with cerebral palsy. Neurosci. Lett. 420 (1), 34–38. http://dx.doi.org/10.1016/j.neulet.2007.04.054.

Son, S.M., Park, S.H., Moon, H.K., Lee, E., Ahn, S.H., Cho, Y.W., Jang, S.H., 2009. Diffusion tensor tractography can predict hemiparesis in infants with high risk factors. Neurosci. Lett. 451 (1), 94–97. http://dx.doi.org/10.1016/j.neulet.2008.12.033.

Thomas, B., Eyssen, M., Peeters, R., Molenaers, G., Van Hecke, P., De Cock, P., Sunaert, S., 2005. Quantitative diffusion tensor imaging in cerebral palsy due to periventricular white matter injury. Brain 128 (Pt 11), 2562–2577. http://dx.doi.org/10.1093/brain/awh600.

Tournier, J.-D., Calamante, F., Connelly, A., 2007. Robust determination of the fibre orientation distribution in diffusion MRI: non-negativity constrained super-resolved spherical deconvolution. NeuroImage 35 (4), 1459–1472. http://dx.doi.org/10.1016/j.neuroimage.2007.02.016.

Tournier, J.-D., Calamante, F., Connelly, A., 2012. MRtrix: diffusion tractography in crossing fiber regions. Int. J. Imaging Syst. Technol. 22 (1), 53–66. http://dx.doi.org/10.1002/ima.22005.

Trivedi, R., Agarwal, S., Shah, V., Goyel, P., Paliwal, V.K., Rathore, R.K.S., Gupta, R.K., 2010. Correlation of quantitative sensorimotor tractography with clinical grade of cerebral palsy. Neuroradiology 52 (8), 759–765. http://dx.doi.org/10.1007/s00234-010-0703-8.

Tsao, H., Pannek, K., Boyd, R.N., Rose, S.E., 2013. Changes in the integrity of thalamocortical connections are associated with sensorimotor deficits in children with congenital hemiplegia. Brain Struct. Funct. http://dx.doi.org/10.1007/s00429-013-0656-.

Vogt, B.A., Vogt, L., Laureys, S., 2006. Cytology and functionally correlated circuits of human posterior cingulate areas. NeuroImage 29 (2), 452–466. http://dx.doi.org/10.1016/j.neuroimage.2005.07.048.

Wheeler-Kingshott, C.A., Cercignani, M., 2009. About "axial" and "radial" diffusivities. Magn. Reson. Med. 61 (5), 1255–1260. http://dx.doi.org/10.1002/mrm.2196.

Yoshida, S., Hayakawa, K., Yamamoto, A., Okano, S., Kanda, T., Yamori, Y., Hirota, H., 2010. Quantitative diffusion tensor tractography of the motor and sensory tract in children with cerebral palsy. Dev. Med. Child Neurol. 52 (10), 935–940. http://dx.doi.org/10.1111/j.1469-8749.2010.03669.x.

Yoshida, S., Hayakawa, K., Oishi, K., Mori, S., Kanda, T., Yamori, Y., Matsushita, H., 2011. Athetotic and spastic cerebral palsy: anatomic characterization based on diffusion-tensor imaging. Radiology 260 (2), 511–520. http://dx.doi.org/10.1148/radiol.11101783.

Zalesky, A., Fornito, A., Bullmore, E.T., 2010. Network-based statistic: identifying differences in brain networks. NeuroImage 53 (4), 1197–1207. http://dx.doi.org/10.1016/j.neuroimage.2010.06.041.